EINDHOVEN UNIVERSITY OF TECHNOLOGY

N, NH, and NH2 radical densities in a remote Ar-NH3-SiH4 plasma and their role in silicon nitride deposition

Citation for published version (APA):
Oever, van den, P. J., Helden, van, J. H., Hemmen, van, J. L., Engeln, R. A. H., Schram, D. C., Sanden, van de, M. C. M., & Kessels, W. M. M. (2006). N, NH, and NH2 radical densities in a remote Ar-NH3-SiH4 plasma and their role in silicon nitride deposition. *Journal of Applied Physics*, *100*(9), 093303-1/10. Article 093303. https://doi.org/10.1063/1.2358330

DOI:
10.1063/1.2358330

Document status and date:
Published: 01/01/2006

Document Version:
Publisher's PDF, also known as Version of Record (includes final page, issue and volume numbers)

Please check the document version of this publication:

• A submitted manuscript is the version of the article upon submission and before peer-review. There can be important differences between the submitted version and the official published version of record. People interested in the research are advised to contact the author for the final version of the publication, or visit the DOI to the publisher's website.
• The final author version and the galley proof are versions of the publication after peer review.
• The final published version features the final layout of the paper including the volume, issue and page numbers.

Link to publication

General rights
Copyright and moral rights for the publications made accessible in the public portal are retained by the authors and/or other copyright owners and it is a condition of accessing publications that users recognise and abide by the legal requirements associated with these rights.

- Users may download and print one copy of any publication from the public portal for the purpose of private study or research.
- You may not further distribute the material or use it for any profit-making activity or commercial gain
- You may freely distribute the URL identifying the publication in the public portal.

If the publication is distributed under the terms of Article 25fa of the Dutch Copyright Act, indicated by the "Taverne" license above, please follow below link for the End User Agreement:

www.tue.nl/taverne

Take down policy
If you believe that this document breaches copyright please contact us at:

openaccess@tue.nl

providing details and we will investigate your claim.

Download date: 04. Oct. 2023

N, NH, and NH_2 radical densities in a remote $Ar-NH_3-SiH_4$ plasma and their role in silicon nitride deposition

P. J. van den Oever,[a] J. H. van Helden, J. L. van Hemmen, R. Engeln, D. C. Schram, M. C. M. van de Sanden, and W. M. M. Kessels[b]
Department of Applied Physics, Eindhoven University of Technology, P.O. Box 513, 5600 MB Eindhoven, The Netherlands

(Received 28 May 2006; accepted 27 July 2006; published online 6 November 2006)

The densities of N, NH, and NH_2 radicals in a remote $Ar-NH_3-SiH_4$ plasma used for high-rate silicon nitride deposition were investigated for different gas mixtures and plasma settings using cavity ringdown absorption spectroscopy and threshold ionization mass spectrometry. For typical deposition conditions, the N, NH, and NH_2 radical densities are on the order of 10^{12} cm^{-3} and the trends with NH_3 flow, SiH_4 flow, and plasma source current are reported. We present a feasible reaction pathway for the production and loss of the NH_x radicals that is consistent with the experimental results. Furthermore, mass spectrometry revealed that the consumption of NH_3 was typically 40%, while it was over 80% for SiH_4. On the basis of the measured N densities we deduced the recombination and sticking coefficient for N radicals on a silicon nitride film. Using this sticking coefficient and reported surface reaction probabilities of NH and NH_2 radicals, we conclude that N and NH_2 radicals are mainly responsible for the N incorporation in the silicon nitride film, while Si atoms are most likely brought to the surface in the form of SiH_x radicals. © *2006 American Institute of Physics*. [DOI: 10.1063/1.2358330]

I. INTRODUCTION

Plasma deposited amorphous silicon nitride (a-SiN_x:H) thin films have been studied extensively because of their electrical and optical properties that make them very suitable for many applications in microelectronics device fabrication (e.g., as gate dielectric or passivation layer).[1–3] Other applications can be found in the encapsulation of devices such as organic light emitting devices[4] and in the photovoltaic industry, where a-SiN_x:H is used as an antireflection coating on c-Si solar cells that also serves as a surface and bulk passivation layer to improve the carrier lifetime in silicon.[5,6] Most silicon nitride deposition processes use mixtures of SiH_4 and NH_3 or N_2, but also liquid precursors such as hexamethyldisilazane (HMDS), tris(diethylamino)chlorosilane (TDEACS), and bis(dimethylamino)-dimethylsilane (BDMADMS) have been used with varying success.[7–9]

Because of their numerous applications, silicon nitride films deposited by plasma enhanced chemical vapor deposition (PECVD) have been widely investigated and the dependence of the film properties on the plasma gas composition and deposition conditions was established in various types of plasma reactors.[10–13] However, due to the complexity of chemical reactions both in the gas phase and at the surface, the mechanisms underlying silicon nitride deposition are not yet fully understood and further knowledge of the processes taking place in the plasma is still required. For N_2-SiH_4 plasmas several studies of the silicon nitride growth mechanism were reported. In 1990 Smith *et al.* found that N radicals are probably directly incorporated in the a-SiN_x:H film,[14] while Hanyaloglu and Aydil (1998) suggested on the basis of optical emission spectroscopy that excited N_2^* molecules are most likely responsible for the N incorporation in the a-SiN_x:H films.[15] Recently, more support for the incorporation of N radicals in the a-SiN_x:H film was found in a remote $Ar-N_2-H_2-SiH_4$ plasma and a refined growth mechanism was proposed. In this refined growth mechanism an a-Si:H-like surface layer formed by predominantly SiH_3 radicals is converted into a-SiN_x:H by nitridation reactions with impinging N radicals.[16,17]

On the other hand, Smith *et al.*[11,18] identified the amino-silane radical as the most important precursor for silicon nitride deposition in a NH_3-SiH_4 radio frequency plasma using mass spectrometry. This result was supported by Beach and Jasinski (1990) who proposed a reaction mechanism for the formation of amino-silane radicals involving NH_2 radicals.[19] In 1995, Murley *et al.* showed that the amount of amino-silanes formed is dependent on the gas residence time inside the reactor chamber.[20] Long residence times typically lead to high amino-silane concentrations, whereas short residence times result in no amino-silanes at all, which suggests the existence of a complementary growth mechanism most likely based on SiH_x and NH_x radicals under short-residence-time conditions.

For a-SiN_x:H growth based on NH_3-SiH_4 gas mixtures, the role and densities of N, NH, and NH_2 radicals were not yet investigated in great detail. The results of Theil *et al.* (1992) suggest that SiH_x and NH_x radicals are more important for silicon nitride growth than the amino-silane radicals,[21] although they did not measure these radicals directly. More recently Umemoto *et al.* measured NH, NH_2, and SiH_3 radicals in a hot wire chemical vapor deposition (CVD) process and they found that SiH_3 and NH_2 are most

[a]Electronic mail: p.j.v.d.oever@tue.nl
[b]Author to whom correspondence should be addressed; electronic mail: w.m.m.kessels@tue.nl

0021-8979/2006/100(9)/093303/10/$23.00

© 2006 American Institute of Physics

Downloaded 14 Sep 2007 to 131.155.108.71. Redistribution subject to AIP license or copyright, see http://jap.aip.org/jap/copyright.jsp

likely responsible for the Si and N incorporations in the film.[22] The density and role of N radicals in NH_3-SiH_4 based plasmas, however, are not well known as limited studies into this subject have been reported.

Further insight into the silicon nitride growth mechanism can be inferred from the interaction of the various NH_x radicals with the surface, which was studied by several research groups. Fisher and co-workers measured the surface interaction of NH and NH_2 radicals for different types of surfaces using laser induced fluorescence combined with a molecular beam setup.[23–25] For N radicals on stainless steel and silicon nitride surfaces, the surface reactivity has been summarized and extended by Kessels *et al.*[17] based on the experimental results of Adams and Miller[26] and Singh *et al.*[27]

In this paper, we report the densities of the NH_x radicals in a remote $Ar-NH_3-SiH_4$ plasma and we focus on the role of these radicals in the deposition process of silicon nitride. In Sec. II, the expanding thermal plasma (ETP) technique operated on an $Ar-NH_3$ gas mixture[28] is briefly described. This technique was recently introduced in industry[29,30] and is capable of depositing good quality silicon nitride at nominal deposition rates ranging from 4 to 7 nm/s, which is faster than most conventional processes (<1 nm/s). The diagnostic techniques, such as cavity ringdown absorption spectroscopy (CRDS) for the detection of NH and NH_2 radicals and threshold ionization mass spectrometry (TIMS) for the N radical measurements, are described briefly in Sec. III. In Sec. IV, we present the NH_x radical densities as function of several plasma parameters such as NH_3 flow, SiH_4 flow, and plasma source current (Secs. IV A–IV C) and discuss the most important plasma reactions that can explain the observed trends. Furthermore, the NH_3 and SiH_4 consumptions and the production of molecules from the dissociated molecules (Sec. IV D) are addressed for different plasma settings. Subsequently, Sec. V summarizes the plasma chemistry and discusses the surface reaction probability of the NH_x radicals and the implications of our measurements on the silicon nitride growth mechanism. Finally, the conclusions are given in Sec. VI.

II. THE EXPANDING THERMAL PLASMA ON AR–NH_3

Figure 1 shows a schematic overview of the deposition setup including the laser setup used for the measurements of the NH and NH_2 densities and the mass spectrometry setup for the determination of the N density. Both diagnostic techniques will be discussed in greater detail in Sec. III.

An extensive description of the plasma source and the ETP technique can be found elsewhere[28,31,32] and here a brief summary of the ETP plasma operated on an $Ar-NH_3$ mixture will be given. The ETP technique consists of a cascaded arc plasma source that operates at subatmospheric pressures (~200 Torr) and a low pressure processing chamber. A dc current of typically 45 A is used to efficiently ionize argon atoms in a narrow plasma channel with flowing argon gas. NH_3 gas is introduced through a slit in the nozzle at the outlet of the plasma source (see Fig. 1) and the resulting $Ar-NH_3$ plasma expands into the low pressure chamber (~0.15 Torr). The electron temperature is low (0.2–0.3 eV)

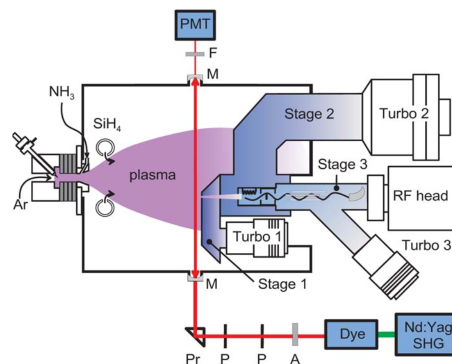

FIG. 1. (Color online) The experimental setup, showing the cascaded arc plasma source, the cavity ringdown setup, and the threshold ionization mass spectrometer. In the figure "F" stands for filter, "M" for mirror, "Pr" for prism, "P" for pinhole and "A" for attenuator.

in the expansion and as a consequence, electron impact induced chemistry and ion bombardment due the plasma self-bias potential are not important. The most important reactive species emanating from the plasma source are Ar^+ ions that transfer their charge to NH_3 molecules in the course of the expansion, creating mainly NH_3^+ molecular ions. These molecular ions recombine dissociatively with electrons into mainly N and NH radicals.[33] The charge transfer reaction as well as the dissociative recombination reaction are very fast and the N and NH densities both saturate at a level of 3×10^{12} cm^{-3} for NH_3 flows above 3 SCCS (standard cubic centimeter per second) due to the limited amount of Ar^+ ions available. Langmuir probe measurements carried out at 36 cm from the plasma source revealed an exponential decrease of the ion density by three orders of magnitude until 3 SCCS NH_3 was injected in the plasma,[28] which is in line with the constant N and NH densities above 3 SCCS NH_3. The saturation also implies that gas phase loss with NH_3 can be neglected for these radicals. NH_2 radicals, on the other hand, are most likely produced differently via reactions of NH_3^+ with NH_3 or via NH_3 dissociation reactions by H abstraction, resulting in a linear increase of the NH_2 density as a function of the NH_3 flow. The NH_2 density reached for 15 SCCS injected NH_3 flow is approximately 4.0×10^{12} cm^{-3}. More information on the reaction mechanism responsible for the creation of NH and NH_2 in the $Ar-NH_3$ plasma can be found in Ref. 33.

When the plasma is used for silicon nitride deposition SiH_4 gas is injected through a ring situated at a distance of approximately 7 cm from the nozzle. The reactive fragments (NH_x, H, etc.) created in the initial part of the expansion are used to dissociate the injected SiH_4 leading to silicon containing reactive species that deposit an a-SiN_x:H film on a downstream situated substrate. The standard experimental conditions and the parameter range used in this study are given in Table I.

III. PLASMA DIAGNOSTICS

A. Cavity ringdown absorption spectroscopy

The cavity ringdown setup is shown schematically in Fig. 1. Laser pulses generated by a dye laser pumped by the

Downloaded 14 Sep 2007 to 131.155.108.71. Redistribution subject to AIP license or copyright, see http://jap.aip.org/jap/copyright.jsp

TABLE I. The range of plasma parameters used in this study.

Parameter	Standard value	Range studied
Ar flow	55 SCCS	⋯
NH_3 flow	17 SCCS	0–17 SCCS
SiH_4 flow	2.5 SCCS	0–5 SCCS
Arc current	45 A	30–70 A
Arc voltage	42 V	⋯
Arc pressure	210 Torr	⋯
Downstream pressure	0.15 Torr	⋯

second harmonic radiation of a Nd:YAG (yttrium aluminum garnet) laser were injected into a high finesse optical cavity formed by two planoconcave high reflectivity mirrors (M). The mirrors, protected from reactive plasma species by a small argon flow, were placed 112 cm apart on flexible bellows at a distance of 36 cm from the plasma source, which is 3 cm before the substrate holder. Before injection into the cavity, the laser pulse energy was attenuated to below 100 μJ per pulse to avoid optical saturation of the used transitions. The light intensity leaking out of the cavity was detected through an interference bandpass filter (F) by a photomultiplier tube (PMT). For every single laser pulse, the decay rate was sampled by a 100 MHz, 12 bit data acquisition system [TU/eDACS (Ref. 34)]. All observed decay rates were single exponential and were analyzed by a weighted least squares fit of the logarithmic of the transient data, while an average of 20 single decays was used to improve the signal to noise ratio. More details on the cavity ringdown setup can be found elsewhere.[33]

The NH radical was detected on the (0,0) band of the $A\,^3\Pi \leftarrow X\,^3\Sigma^-$ transition around ~340 nm and the NH_2 radical on the (0,9,0)-(0,0,0) band of the $\tilde{A}\,^2A_1 \leftarrow \tilde{X}\,^2B_1$ transition at ~597 nm. For NH, the isolated $P_{3,3}(9)$ absorption line at 339.624 nm (29 444.3 cm^{-1}) was used, while the "isolated" $\Sigma^P Q_{1,7}$ absorption line at 597.375 nm (16 739.9 cm^{-1}) was used for NH_2. The actual density information was determined by scanning the laser over the particular absorption line and using the integrated absorption cross sections derived in Ref. 33.

First, the spectra of NH and NH_2 were recorded for the $Ar-NH_3$ plasma to establish the measurement procedure. We found that the addition of SiH_4 to the plasma introduced a broadband absorption in addition to the NH and NH_2 spectral features. The origin of this broadband absorption has not been identified, but it did not change the distinct spectral features of the NH and NH_2 radicals. The largest uncertainty in the absolute values of the densities reported is generated by the assumption about the absorption path length for the radicals in the plasma, which is estimated to be 30 cm.[35] This systematic error can be as large as a factor of 3 for the local absolute densities.

B. (Threshold ionization) mass spectrometry

The triple stage differentially pumped quadrupole mass spectrometer (QMS) used in this study was modified from the version that was used to measure N radicals in an $Ar-N_2-SiH_4$ plasma.[16] The apparatus used in this study is

TABLE II. Various reactions leading to N^+ ions in the mass spectrometer's ionizer by electron impact ionization. The corresponding appearance potentials are also given.

	Reaction	Appearance potential (eV)	Ref.
A	$N+e \rightarrow N^+ + 2e$	15.3	a
B	$NH_3+e \rightarrow N^+ + H_2 + H + 2e$	22.6	b
C	$N_2+e \rightarrow N^+ + N + 2e$	24.3	b

[a]Reference 46.
[b]Reference 47.

based on the design by Agarwal *et al.*[36] and was described extensively elsewhere.[28,37] Briefly, the plasma is sampled by effusive extraction through a 0.8 mm orifice that is situated approximately 56 cm from the plasma source and 4.5 cm off the reactor axis. The extraction creates a molecular beam that passes two consecutive orifices separating the pumping stages in the housing of the mass spectrometer. The quadrupole mass spectrometer (Hiden Analytical Epic 300, PSM upgrade) is placed in the third stage, in line of sight with the three orifices. Typical pressures in the second and third stages during measurements are 10^{-6} and 10^{-7} Torr, respectively, while the third stage base pressure is below 10^{-9} Torr. Due to the finite pressure in the third stage, the mass spectrometer signal will not only consist of a beam component but also of a background component due to surface scattered molecules.

Ground state N radicals were detected using the so-called threshold ionization or appearance potential technique.[14,28] In general, electron impact ionization of radicals has a lower threshold than dissociative ionization of parent molecules leading to the same ion. Table II shows the different electron impact ionization processes that lead to the detection of an ion with a mass-over-charge (m/e) ratio equal to 14. By scanning the electron energy used for ionization, we can distinguish different ionization processes. To obtain absolute densities of N radicals, we used a calibration method for the N radicals similar to the one described by Singh *et al.*[27] The absolute N densities were obtained by correlating the measured signal of N radicals to the direct ionization signal of NH_3 reference gas with a known number density. The details of the calibration procedure can be found in Ref. 28.

The mass spectrometer was also used to determine the densities of stable species such as NH_3, SiH_4, H_2, and N_2 in the plasma beam. The calibration procedure to obtain the absolute densities of these molecules was carried out prior to each measurement run using different reference gas mixtures in argon (e.g. NH_3 in Ar, SiH_4 in Ar, etc.) to mimic the actual measurement conditions. From these measurements the relative consumption or depletion of a species can be calculated.

For the $Ar-NH_3-SiH_4$ plasma, all signals were corrected for clogging of the sampling orifice by normalizing all signals to the Ar signal in the "plasma off" case. This correction was not necessary for non-depositing plasmas.

Downloaded 14 Sep 2007 to 131.155.108.71. Redistribution subject to AIP license or copyright, see http://jap.aip.org/jap/copyright.jsp

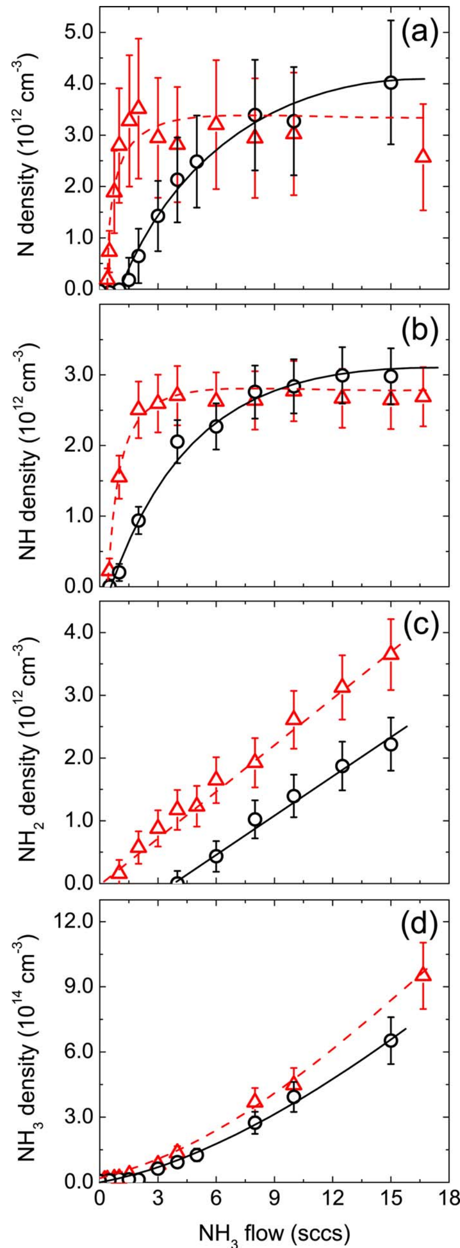

FIG. 2. (Color online) The N (a), NH (b), NH_2 (c), and NH_3 (d) densities as a function of the NH_3 flow for an injected SiH_4 flow of 0 SCCS (open triangles, dashed line) and 2.5 SCCS (open circles, solid line). The arc current was 45 A. The N and NH_3 densities were measured by (threshold ionization) mass spectrometry and the NH and NH_2 densities by cavity ringdown spectroscopy. The lines serve as a guide to the eyes.

IV. RESULTS

A. NH_x radical densities versus NH_3 flow

Figures 2(a)–2(d) show the absolute densities of N, NH, and NH_2 radicals and NH_3 molecules in the expanding $Ar-NH_3-SiH_4$ plasma as a function of the NH_3 flow for a SiH_4 flow of 2.5 SCCS (circles). The observed trends for a pure $Ar-NH_3$ plasma (described in Sec. II) are also shown for comparison (triangles). When 2.5 SCCS SiH_4 is added to the $Ar-NH_3$ plasma, the behavior of the NH_x ($x=0-3$) densities is quite similar to the situation without SiH_4 as can be seen in Fig. 2. The N and NH densities increase more gradual to their final values of $\sim 4.0\times 10^{12}$ and $\sim 3.0 \times 10^{12}$ cm^{-3}, respectively. Also the NH_2 density shows a similar linear increase as in the case without SiH_4 reaching a density of 2.5×10^{12} cm^{-3} at 15 SCCS NH_3. For NH_3 flows below 4 SCCS, however, no NH_2 radicals could be detected in the plasma in contrast to the situation without SiH_4. The NH_3 density obtained for 15 SCCS NH_3 flow is 7.0 $\times 10^{14}$ cm^{-3}, which is slightly lower than in the situation without SiH_4.

The observed density changes can be qualitatively understood by looking at the production rate P and and loss time τ of species in a steady state situation,

$$\frac{\partial n}{\partial t} = P - \frac{n}{\tau} = 0, \tag{1}$$

with n the density of the species. In this case, the observed *gradual* increase of the N and NH densities can be explained by a decrease in the production rate of these radicals due to SiH_4 injection. Competition between charge transfer reactions of Ar^+ ions with NH_3, responsible for the creation of N and NH radicals, and with SiH_4 results in a lower production rate for N and NH. This effect is especially important when the NH_3 flow is comparable to or smaller than the SiH_4 flow, as is also observed in Figs. 2(a) and 2(b). For high NH_3 flows the influence of the charge transfer reaction of Ar^+ with SiH_4 is of minor importance and the observed N and NH densities are similar to the values obtained in the situation without SiH_4. The final N radical density seems to be somewhat higher in the presence of SiH_4, which is predominantly caused by a change in the loss time of the N radical [e.g., a different surface reaction probability (see Sec. V B)]. The absence of NH_2 radicals in the $Ar-NH_3-SiH_4$ plasma for flows below 4 SCCS NH_3 is another indication that the production and/or loss mechanism of NH_2 is different than that of N and NH. Additional measurements showed that the NH_3 flow threshold for NH_2 detection depends linearly on the SiH_4 flow. This behavior is not completely understood yet, but a few mechanisms changing the production or the loss time of NH_2 radicals can be suggested. A first possibility is the abstraction reaction between atomic H and SiH_4. This reaction is much faster at 1750 K (Ref. 33) [reaction rate of $\sim 8\times 10^{-11}$ cm^3 s^{-1} (Ref. 38)] than the equivalent reaction with NH_3 [with a rate of $\sim 3\times 10^{-11}$ cm^3 s^{-1} (Ref. 33)] such that the NH_2 *production* might be suppressed. Another reaction that can play a role is a fast *gas phase loss* reaction of the produced NH_2 with SiH_4 or its dissociation products. Likely candidates for this reaction are the amino-silane creation reactions as proposed by Beach and Jasinski.[19] Finally, NH_2 radicals might be preferentially incorporated in the a-SiN_x:H film leading to the low NH_2 density in the plasma. This argument is supported by values of the NH_2 surface loss probability as discussed in Sec. V B.

B. NH_x radical densities versus SiH_4 flow

The N, NH, and NH_2 radical densities as well as the NH_3 density were also measured for different SiH_4 flows, as shown in Fig. 3. The NH_3 flow was 17 SCCS and the plasma source current was 45 A. The densities of all NH_x radicals decrease significantly when silane is injected in the plasma.

Downloaded 14 Sep 2007 to 131.155.108.71. Redistribution subject to AIP license or copyright, see http://jap.aip.org/jap/copyright.jsp

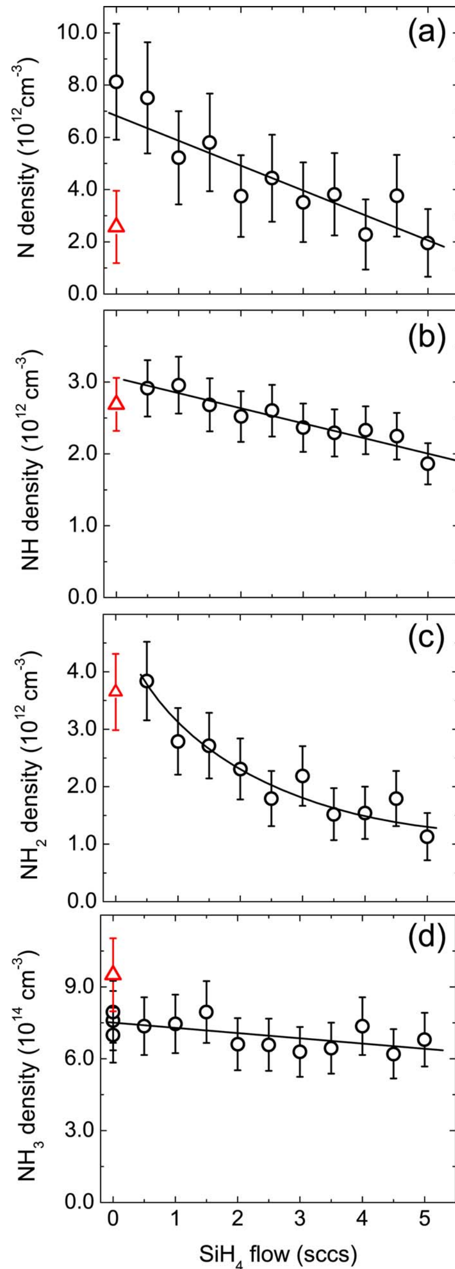

FIG. 3. (Color online) The N (a), NH (b) NH_2 (c), and NH_3 (d) densities as a function of the injected SiH_4 flow for an NH_3 flow of 17 SCCS and an arc current of 45 A. The lines serve as a guide to the eyes. The triangles are the measured values for an Ar–NH_3 plasma with clean stainless steel reactor walls.

The N radical density decreases from $\sim 8.0\times 10^{12}$ to $\sim 2.0\times 10^{12}$ cm^{-3} and the NH density from $\sim 3.0\times 10^{12}$ to $\sim 2.0\times 10^{12}$ cm^{-3}. The NH_2 density decreases from $\sim 4.0\times 10^{12}$ to $\sim 1.0\times 10^{12}$ cm^{-3} for a SiH_4 flow of 5 SCCS, while the NH_3 density decreases only slightly from $\sim 7.5\times 10^{14}$ to $\sim 6.5\times 10^{14}$ cm^{-3}. Figure 3 also shows the values of the NH_x densities in the absence of SiH_4 for a clean stainless steel reactor (open triangles). Note that for small injected SiH_4 flows the N radical density in the depositing plasma is higher than in the situation without SiH_4. This particular behavior will be addressed in more detail in Sec. V B, but first the NH_x radical densities will be discussed in detail.

The small decrease of the NH density versus the SiH_4 flow can be explained by a decreased production rate due to the competition between the Ar^+ charge transfer reactions with NH_3 and SiH_4, as explained in the previous section. The N and NH_2 densities, however, decrease faster than the NH density upon injection of SiH_4, which suggests that an additional *loss* mechanism related to SiH_4 lowers the N and NH_2 densities. A similar decreasing trend for the N radical density versus SiH_4 flow was observed by Kessels *et al.* in an Ar–N_2–H_2–SiH_4 plasma.[16] Due to the endoergic nature of the reaction of N radicals with SiH_4 (enthalpy=+0.45 eV), the corresponding reaction rate is very low at room temperature ($<8\times 10^{-14}$ cm^3 s^{-1}).[39] At a gas temperature of 1750 K, we still expect the reaction rate to be very small due to the relatively high energy barrier for this reaction. Therefore, Kessels *et al.* argued that gas phase loss of N radicals can be excluded and it was established that a larger fraction of N radicals must be incorporated in the a-SiN$_x$:H film. Also for the Ar–NH_3–SiH_4 plasma N incorporation in the a-SiN$_x$:H film is most likely responsible for the observed N loss. For NH_2, a gas phase loss mechanism involving SiH_4 molecules cannot be excluded on the basis of the reaction rates reported in the literature. Two possible reactions that might explain the observed NH_2 loss were already proposed in Sec. IV A. The first reaction, which removes atomic H from the plasma by a reaction with SiH_4 suppressing the NH_2 production, can in principle take place. But on the basis of the small amount of injected SiH_4 molecules, it is unlikely that this reaction can explain the total NH_2 decrease. The second reaction resulting in the creation of amino silanes is not expected to be significant as we found no evidence for these fragments by mass spectrometry. Moreover, a similar decrease of the NH and NH_2 densities versus SiH_4 flow in a hot wire CVD system was attributed to a decreased decomposition efficiency of NH_3 on the hot wire surface[22] and not to gas phase reactions. In our case, the faster decrease of the NH_2 density is presumably caused by an increased incorporation of NH_2 into the a-SiN$_x$:H film at higher SiH_4 flows, similar to the situation for N radicals (Sec. V B).

C. NH_x radical densities versus arc current

Another important plasma parameter, besides the NH_3 and SiH_4 gas flows, is the plasma source current, which determines the amount of ions emanating from the source. Figures 4(a)–4(d) show the NH_x (0–3) densities as a function of the arc current for a NH_3 flow of 17 SCCS and a SiH_4 flow of 2.5 SCCS. The N density increases linearly from $\sim 2.5\times 10^{12}$ to $\sim 9.0\times 10^{12}$ cm^{-3} when the arc current is increased from 30 to 70 A. Also the NH density increases linearly from $\sim 2.0\times 10^{12}$ to $\sim 4.0\times 10^{12}$ cm^{-3}, while the NH_2 density remains almost constant at 2.0×10^{12} cm^{-3}. The NH_3 density in the plasma decreases from $\sim 10.0\times 10^{14}$ to $\sim 4.0\times 10^{14}$ cm^{-3} when the arc current increases from 30 to 70 A.

The linear increase of the N and NH densities versus arc current confirms that the production mechanism of these radicals is dependent on Ar^+ ions from the plasma source, as discussed briefly in Sec. II. The stronger increase of the N density compared to the NH density indicates that N radicals might also be produced in secondary reactions of Ar^+ ions

Downloaded 14 Sep 2007 to 131.155.108.71. Redistribution subject to AIP license or copyright, see http://jap.aip.org/jap/copyright.jsp

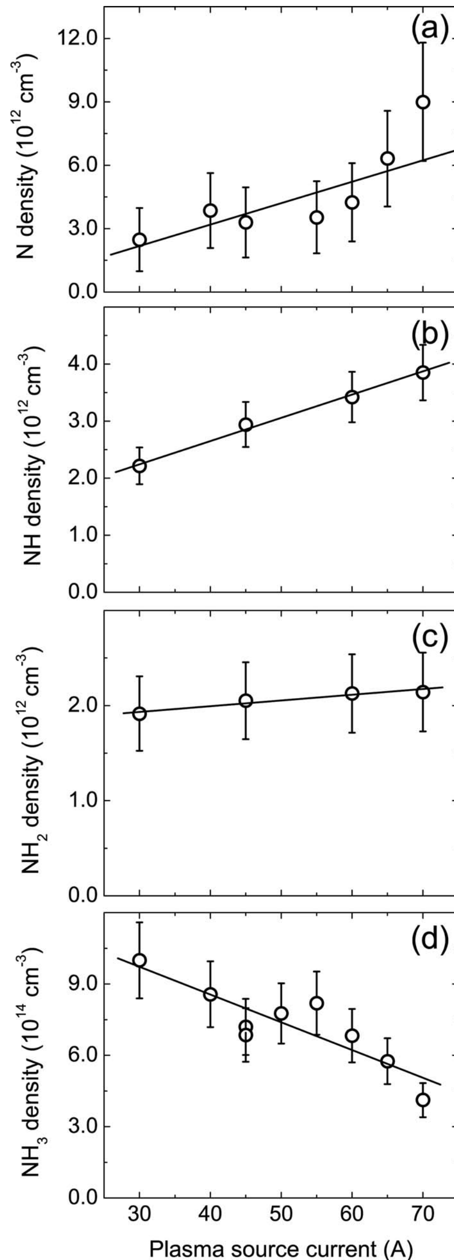

FIG. 4. The N (a), NH (b), NH_2 (c), and NH_3 (d) densities as a function of the arc current for a NH_3 flow of 17 SCCS and a SiH_4 flow of 2.5 SCCS. The lines serve as a guide to the eyes.

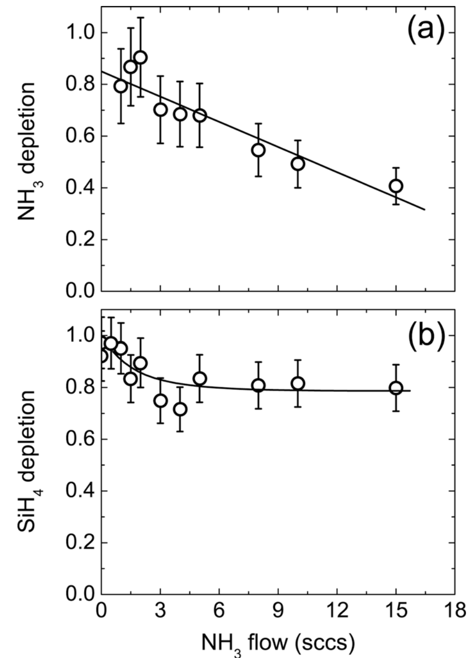

FIG. 5. The depletion of NH_3 (a) and SiH_4 (b) in the Ar–NH_3–SiH_4 plasma vs the NH_3 flow for a SiH_4 flow of 2.5 SCCS. The arc current was 45 A. The lines serve as a guide to the eyes.

with NH_x radicals or N_2 molecules, while this is not the case for NH radicals. The linear decrease in the NH_3 density is expected because the NH_3 dissociation process starts with the charge transfer reaction of Ar^+ with NH_3. Furthermore, the constant NH_2 density corroborates the previous conclusion that NH_2 is produced by a different pathway than N and NH radicals.

D. NH_3 and SiH_4 consumption

The relative amount of gas phase consumption of a precursor, also called depletion, can give valuable insights into the deposition process. Furthermore, an effective use of the precursor gas is important from a cost perspective (e.g., high depletion values allows for more efficient use of precursor gases). The amount of NH_3 and SiH_4 consumed in the plasma can be derived from mass spectrometry measurements of the NH_3 density and SiH_4 density (see Sec. III C). In Fig. 5 we show the depletion of NH_3 (a) and of SiH_4 (b) in the plasma as a function of the NH_3 flow for a SiH_4 flow of 2.5 SCCS. The depletion of NH_3 decreases from ~0.9 for small NH_3 flows to ~0.4 for high NH_3 flows. Accurate measurements of depletions near 100% for low NH_3 flows are difficult, which explains the larger error bars in Fig. 5. The behavior of the NH_3 depletion versus NH_3 flow can be understood by considering the amount of reactive species from the source compared to the injected NH_3 flow and the remote character of the ETP technique.[32] For low NH_3 flows the amount of Ar^+ from the plasma source is sufficient to dissociate all NH_3, but when the NH_3 flow is increased further, the amount of Ar^+ will be deficient to dissociate all NH_3. At this point the depletion of NH_3 starts to decrease. Also the depletion of SiH_4 decreases from ~1.0 to ~0.8 when the NH_3 flow increases from 0 to ~6 SCCS, whereas it remains constant at ~0.8 for higher NH_3 flows. The decrease of the SiH_4 depletion when the NH_3 flow increases is most probably related to a decrease in the direct dissociation of SiH_4 by Ar^+ due to competition of this process with the charge exchange reaction of NH_3 with Ar^+ as discussed in Sec. IV A. At a NH_3 flow of 6 SCCS, most Ar^+ ions are used to dissociate NH_3, while SiH_4 is presumably dissociated indirectly by reactive NH_x species leading to a SiH_4 depletion of ~0.8.

Figures 6(a) and 6(b) show the NH_3 and SiH_4 depletions versus the SiH_4 flow in an Ar–NH_3–SiH_4 plasma for a NH_3 flow of 17 SCCS. The NH_3 depletion remains constant at ~0.4 over the whole range of SiH_4 flows, because the injected SiH_4 flow is relatively small compared to the NH_3 flow. Furthermore, the NH_3 flow is injected in an earlier stage of the plasma expansion than SiH_4 (see Fig. 1). There-

Downloaded 14 Sep 2007 to 131.155.108.71. Redistribution subject to AIP license or copyright, see http://jap.aip.org/jap/copyright.jsp

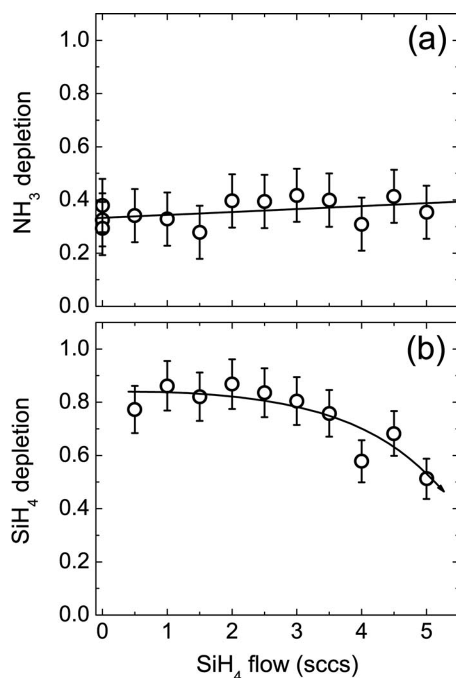

FIG. 6. The depletion of NH_3 (a) and SiH_4 (b) in the $Ar-NH_3-SiH_4$ plasma vs the SiH_4 flow for a NH_3 flow of 17 SCCS. The arc current was 45 A. The lines serve as a guide to the eyes.

fore, the NH_3 dissociation is not affected by the injected SiH_4 flow for these large NH_3 flows. The SiH_4 depletion remains constant at ~0.8 for SiH_4 flows between 0 and 2.5 SCCS SiH_4 and subsequently decreases to ~0.5 for a SiH_4 flow of 5 SCCS. This suggests that the amount of reactive species created in the NH_3 dissociation process is the limiting factor for the SiH_4 dissociation for SiH_4 flows exceeding 2.5 SCCS.

In the expanding thermal plasma, the NH_3 depletion is in the order of 40% for actual deposition conditions of silicon nitride antireflection coatings on solar cells, while the SiH_4 depletion is approximately 80%. Note that the consumed NH_3 flow is actually larger than the consumed SiH_4 flow leading to near stoichiometric silicon nitride. These values for the NH_3 and SiH_4 depletions are relatively high in comparison to the results reported by Umemoto *et al.* They reported a NH_3 depletion of 5% and a SiH_4 depletion of 60% in the hot wire CVD process based on NH_3 and SiH_4. However, when H_2 is added to the NH_3/SiH_4 system, a much higher NH_3 decomposition efficiency can be achieved in the hot wire CVD process.[40–42] Chowdhury *et al.* reported SiH_4 depletions up to 100% for small SiH_4 flows and high power density in their rf PECVD system based on N_2 and SiH_4.[43] In the ETP plasma, both the NH_3 and the SiH_4 depletions increase when the arc current and therefore the plasma power are increased. For an injected SiH_4 flow of 2.5 SCCS, NH_3 flow of 17 SCCS, and an arc current of 70 A, the NH_3 and SiH_4 depletions are ~60% and ~100%, respectively. These high values of the depletion enable high rate deposition of a-SiN_x:H using the ETP technique.

The typical depleted NH_3 density when the plasma is switched on is on the order of 10^{14} cm^{-3} while the typical NH_x densities generated are on the order of 10^{12} cm^{-3} during actual deposition conditions. The difference in magnitude of these densities cannot be explained by N or H incorporation in the film alone, which means that other species besides NH_x radicals must be generated in the plasma. For an $Ar-NH_3$ plasma, it was already demonstrated that large densities of N_2 and H_2 molecules were generated.[28] Also in the $Ar-NH_3-SiH_4$ plasma we observed that most of the depleted NH_3 and SiH_4 flows are converted into H_2 and N_2 with typical densities on the order of 10^{14} cm^{-3} (not shown). A similar observation was also reported by Umemoto *et al.*, who measured the H_2 and N_2 productions in their hot wire CVD system.

V. DISCUSSION

A. Summary of the plasma chemistry

From the results presented in the current study combined with the outcome of previous studies, the following reaction pathway in the $Ar-NH_3-SiH_4$ plasma can be deduced. The cascaded arc plasma source produces primarily Ar^+ ions that undergo a charge transfer reaction with NH_3 molecules injected in the very first part of the plasma expansion. The NH_3^+ ions created recombine dissociatively into N and NH radicals, while NH_2 radicals are produced via ion-molecule reactions or radical-molecule reactions with NH_3 molecules. This mechanism leads to relatively high N and NH densities that saturate at a level of $(3.0-4.0)\times 10^{12}$ cm^{-3} for high NH_3 flows due the limited amount of Ar^+ available. The NH_2 density on the other hand increases linearly with the NH_3 flow and reaches a level of 2.5×10^{12} cm^{-3}.

When SiH_4 is injected in the plasma all NH_x radicals decrease in density. For a part, this decrease can be explained by a lower production rate due to the competition between the charge transfer reaction of Ar^+ with NH_3 and the charge transfer reaction of Ar^+ with SiH_4. However, for the N and NH_2 radicals the decrease in density is more pronounced than for the NH radical suggesting that an additional loss mechanism is present for the N and NH_2 radicals, besides the reduction of their production rate. This loss mechanism is most likely an increased incorporation of these radicals in the a-SiN_x:H film, as can be concluded from the surface loss of these radicals that will be discussed in Sec. V B. In this case, the Si–N bond characteristic for a-SiN_x:H is *not* predominantly formed in the plasma volume, but on the surface of the growing film. When the SiH_4 flow injected in the plasma is increased, the surface composition of the growing film changes due to a higher flux of impinging SiH_x radicals that create additional sites for N incorporation on the film's surface. Therefore, the surface loss rate of N radicals will increase for higher SiH_4 flows.

The amount of reactive species emanating from the plasma source can be increased by a higher current, which leads to more production of N and NH radicals and a higher NH_3 consumption in the plasma. The higher flow of reactive NH_x species from the plasma source also allows for a higher degree of SiH_4 dissociation. For a plasma with a NH_3 flow of 17 SCCS, a SiH_4 flow of 2.5 SCCS, and a plasma source current of 70 A, the dissociation degree of NH_3 and SiH_4 can be as high as 60% and 100%, respectively. Finally, it was

Downloaded 14 Sep 2007 to 131.155.108.71. Redistribution subject to AIP license or copyright, see http://jap.aip.org/jap/copyright.jsp

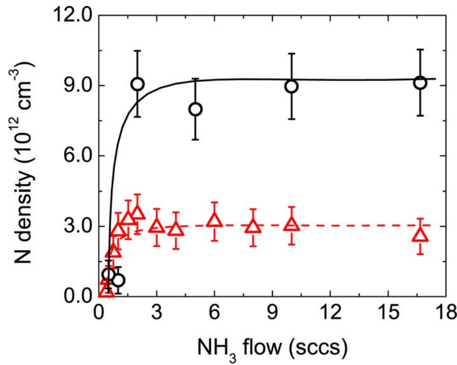

FIG. 7. (Color online) The N radical density vs the NH_3 flow measured in an Ar-NH_3 plasma by threshold ionization mass spectrometry for clean stainless steel reactor walls (triangles) and silicon nitride covered reactor walls (circles). The plasma settings were equal in both cases. The lines serve as a guide to the eyes.

observed that significant amounts of N_2 and H_2 molecules are produced in the plasma from dissociated NH_3 and SiH_4.

B. Surface loss probabilities

The kinetics of film growth in a plasma depend on the interactions of the plasma-generated species with the growing film surface. In order to understand how the film composition and electronic properties are related to the plasma parameters, detailed information on the interaction of the plasma species with the surface is required.

Information on the surface reactivity of species can be deduced from density measurements for different wall conditions. Figure 7 shows a measurement of the N radical density versus the NH_3 flow in an Ar–NH_3 plasma for a clean stainless steel wall and a wall covered with a silicon nitride film. The observed trends for both curves are identical, but the saturation value of the N radical density is substantially higher for the case of silicon nitride covered walls. For stainless steel walls the measured N density n_{SS} at high NH_3 flows is $\sim 3.0\times 10^{12}$ cm^{-3}, while n_{SiN} is $\sim 9.0\times 10^{12}$ cm^{-3} for walls covered with silicon nitride. This difference in N density was already observed in Fig. 3(a), where the N density for stainless steel walls (triangles) lies considerably lower than the N density in a depositing Ar–NH_3–SiH_4 plasma (circles). Assuming constant production rate (P) and no difference in gas phase loss for N radicals (corroborated by the extremely low reactivity of the N radical with SiH_4), the observed density difference must be caused by a changing surface loss rate [see Eq. (1)]. In general, species can be lost at the surface with a probability β, which consists of a "recombination part" with a probability γ and of a "growth part" with a probability s. According Motz and Wise[44] the flux of species that is lost at the surface is given by

$$\Phi_{\text{loss}} = \frac{nv}{4}\frac{\beta}{1-(\beta/2)}, \tag{2}$$

with $\beta=\gamma+s$, n the density of the species, and v the thermal velocity. In a nondepositing NH_3 plasma, the sticking probability s is zero and the flux of species lost at the surface is determined by the recombination probability γ. For our experimental conditions with a partial N_2 pressure on the order of 10 mTorr, the recombination probability on stainless steel γ_{SS} can be estimated at ~ 0.1 on the basis of the work of Adams and Miller[26] and Singh *et al.*[27] Using this value of γ_{SS} and the experimentally observed density ratio n_{SiN}/n_{SS} of ~ 3.0, we obtain a recombination probability of N radicals on a silicon nitride surface γ_{SiN} of ~ 0.03 via Eq. (2).

In SiH_4 containing plasmas the sticking probability s is nonzero as N radicals can also be incorporated in the growing a-SiN_x:H film. When we attribute the decrease in the N density as a function of the injected SiH_4 flow in Fig. 3(a) solely to N incorporation in the a-SiN_x:H film, we can calculate an upper estimate for the sticking coefficient s, assuming a constant N recombination probability γ_{SiN}, no significant change in the N production rate due to SiH_4 addition, and no gas phase loss. For example, the N density is $\sim 8.0\times 10^{12}$ cm^{-3} for a SiH_4 flow of 0 SCCS, while it is $\sim 6.0\times 10^{12}$ cm^{-3} for a SiH_4 flow of 1 SCCS. In the first situation the loss will only consist of N recombination on the surface ($s=0$), while in the second case incorporation of N in the film causes an additional decrease in the N density. Using Eq. (2) we obtain a sticking coefficient s that varies with SiH_4 flow: from ~ 0.016 for 1 SCCS injected SiH_4 to ~ 0.034 when the SiH_4 flow is 5 SCCS. A similar change in the surface reaction probability $\beta=\gamma+s$ from ~ 0.007 for low SiH_4 flows to ~ 0.04 for higher SiH_4 flows was also observed by Kessels *et al.* in the Ar–N_2–H_2-SiH_4 expanding plasma.[16,17] This change in the sticking probability s for higher SiH_4 flows is most likely caused by a higher SiH_x flux to the surface creating more reactive surface sites available for N incorporation.

For NH and NH_2 radicals no significant difference in the surface recombination probability was observed on the basis of the measured densities in nondepositing plasmas for stainless steel walls and silicon nitride covered walls [see Figs. 3(b) and 3(c)]. The surface reactivity of NH and NH_2 on different materials was reported by Fisher and co-workers using laser induced fluorescence in combination with a molecular beam setup.[23–25] The molecular beam was created from a rf powered plasma based on a NH_3 or NH_3–SiH_4 feed gas mixture by expansion into a differentially pumped reactor. A surface loss probability $\beta_{NH}=0.0\pm 0.1$ for the NH radical on a-SiN_x:H surfaces in NH_3 and NH_3–SiH_4 plasmas was observed,[23] indicating that the NH radical is virtually not reactive with the surface during plasma deposition of a-SiN_x:H ($s_{NH}=0$). For the NH_2 radical, surface production ($\gamma_{NH_2}<0$) was found on a-SiN_x:H surfaces in a NH_3 plasma, while a surface loss probability β_{NH_2} of 0.13 ± 0.07 was found in a NH_3–SiH_4 plasma.[24] This suggests that NH_2 is incorporated in the growing a-SiN_x:H film. Assuming a similar NH_2 recombination probability in NH_3 and NH_3–SiH_4 plasmas, we deduce a sticking coefficient for NH_2 (s_{NH_2}) during a-SiN_x:H growth that is larger than 0.13.

C. Implications for *a*-SiN_x:H growth mechanism

The deposition of a-SiN_x:H films by plasmas is governed by reactive species (radicals) created in the plasma and their reaction kinetics on the surface (See Sec. V B). More specifically, radical species are responsible for the creation of

Downloaded 14 Sep 2007 to 131.155.108.71. Redistribution subject to AIP license or copyright, see http://jap.aip.org/jap/copyright.jsp

the Si–N network and two main options were introduced for the deposition mechanism of these films. One mechanism was proposed by Smith *et al.* and is based on the creation of amino-silane radicals $[Si(NH_2)_3]$ in the plasma phase[11] that are responsible for the a-SiN_x:H growth. On the other hand, Umemoto *et al.*[22] have demonstrated that NH_2 and SiH_3 radicals are the dominant growth precursors in the hot wire CVD deposition process of silicon nitride. These two mechanisms differ in the formation path of the characteristic Si–N bond, e.g., in the gas phase or on the surface of the growing film. In our analysis, we also found no evidence for the existence of amino silanes in the ETP plasma by mass spectrometry, although the presence of the broadband absorption in the cavity ringdown measurements might indicate the presence of larger species. Umemoto *et al.* suggested that the absence of amino silanes in the hot wire CVD process is caused by the relatively high atomic H fluxes that are created in the thermal decomposition of the injected precursors on the hot filament. In the expanding thermal plasma, the production of atomic H is also very efficient via the dissociative recombination reactions of NH_x^+ ions with electrons (see Sec. III A). This could explain the absence of amino silanes in the ETP plasma. Alternatively, Murley *et al.* provided another explanation for the absence of amino silanes, which is related to the residence time of the gas in the reactor.[20] They showed that amino silanes are primarily present for residence times higher than 2–3 s, which is larger than commonly used in the ETP plasma (typically ~0.5 s).

Based on our data of the $Ar-NH_3-SiH_4$ plasma, we conclude that the N incorporation in a-SiN_x:H film is most likely dominated by NH_x radicals, which implies that the Si atoms are brought to the surface via SiH_x radicals. This mechanism of Si incorporation by SiH_x radicals is also dominant in the $Ar-N_2-H_2-SiH_4$ plasma[16] and in the deposition of a-Si:H from $Ar-H_2-SiH_4$ plasmas. In the $Ar-NH_3-SiH_4$ plasma, we have also observed Si, SiH and SiH_3 radicals by TIMS measurements. A preliminary study has shown that the densities of these radicals are all approximately $\sim 10^{11}$ cm^{-3}. From this perspective, it is expected that the role of N radicals in the $Ar-NH_3-SiH_4$ plasma is similar to their role in the silicon nitride growth mechanism from N_2-SiH_4 plasmas proposed by Smith *et al.*[14] and Kessels *et al.*[16,17] They showed that N radicals can insert into Si–Si backbonds of an a-Si:H-like layer that is created by impinging SiH_x radicals. NH radicals on the other hand are not reactive with the growing film, as can be deduced from the measured surface reaction probability, while NH_2 radicals are reactive on the surface with a reaction probability of ~0.13. This value is much higher than the reaction probability of N radicals (<0.04), indicating a different sticking process on the surface of the growing film. NH_2 radicals might stick on dangling bonds on the surface or insert into (strained) Si–Si bonds. Furthermore, NH_2 could diffuse over the growing surface in a sort of hot precursor state, similar to the suggested mechanisms for SiH_3 in a-Si:H growth.[45]

The actual contribution of the NH_x radicals to the silicon nitride growth depends on the measured densities and the surface reactivity of the radicals. These two parameters determine the N incorporation flux in the a-SiN_x:H film. To consider the feasibility of N incorporation by NH_x radicals, we estimate the N incorporation flux in two different ways. The first one is based on the deposition rate and the N atomic density determined from elastic recoil detection (ERD) measurements and in the second one we use the measured NH_x densities, the reported surface reaction probabilities, and the estimated thermal velocity of the radicals in the plasma. For 1 SCCS injected SiH_4, 17 SCCS NH_3, and 45 A arc current, the N atomic density of the film was $\sim 3.8 \times 10^{22}$ cm^{-3} and the deposition rate ~6 nm/s, resulting in a N incorporation flux of 2.3×10^{16} cm^{-2} s^{-1}. For the calculation of the N incorporation flux from the radical densities on the other hand, we assume a sticking probability of ~0.02 for N radicals, ~0 for NH radicals, and ~0.13 for NH_2 radicals based on the discussion in Sec. V B. Now we can calculate the contribution of N, NH, and NH_2 radicals to the growth assuming a thermal velocity of ~1600 m/s (corresponding to a gas temperature of 1750 K (Ref. 33)), resulting in 4.9×10^{15}, 0, and 1.6×10^{16} cm^{-2} s^{-1} for N, NH, and NH_2, respectively. Taking into account the limited experimental accuracy in the sticking probability, the two incorporation fluxes 2.3×10^{16} and 2.1×10^{16} cm^{-2} s^{-1} are in good agreement. Therefore, we conclude that the N incorporation in the a-SiN_x:H film can be explained by the NH_x radical densities and their sticking probabilities. The NH_2 radical is the most important radical for N incorporation in the film (roughly 77%), followed by the N radical (roughly 23%). This result is similar to the growth mechanism based on SiH_3 and NH_2 radicals proposed by Umemoto *et al.* in a hot wire CVD process.

VI. CONCLUSIONS

The densities of N, NH, and NH_2 radicals in the $Ar-NH_3-SiH_4$ expanding thermal plasma used for silicon nitride deposition were investigated. The radicals were measured as a function of several plasma parameters such as NH_3 flow, SiH_4 flow, and arc current. For typical deposition conditions, we found densities of $\sim 5.0 \times 10^{12}$ cm^{-3} for N radicals, $\sim 2.5 \times 10^{12}$ cm^{-3} for NH radicals, and $\sim 2.0 \times 10^{12}$ cm^{-3} for NH_2 radicals. In the SiH_4 containing plasma the densities of N, NH, and NH_2 decrease with increasing SiH_4 flow, with the decrease being more prominent for N and NH_2. For NH, the decrease is most likely only due to a change in the production rate of the radicals, while N and NH_2 radicals decrease also in density as they are incorporated in the a-SiN_x:H film.

Besides the radical densities also the relative consumptions of NH_3 and SiH_4 in the plasma have been measured by mass spectrometry. For NH_3 we found relative consumptions in the range of 90%–40%, while the observed SiH_4 consumption lies between 90% and 60%. A large part of the consumed NH_3 is converted into H_2 and N_2 molecules, as was revealed by the large densities of these molecules (typically 10^{14} cm^{-3}) in the plasma. Also the SiH_4 consumption contributes significantly to the observed H_2 density in the plasma.

Downloaded 14 Sep 2007 to 131.155.108.71. Redistribution subject to AIP license or copyright, see http://jap.aip.org/jap/copyright.jsp

Furthermore, we presented evidence that the recombination probability γ of N radicals is lower on a silicon nitride covered wall than on a stainless steel reactor wall. For NH and NH_2 such a difference in recombination probability was not observed. The sticking probability s for N radicals was also deduced from the measurements and varies with SiH_4 flow from ~0.01 to ~0.04. Comparison of the N growth flux calculated from the N atomic density in the film with the contributions of N, NH, and NH_2 to the growth has led to the conclusion that these radicals can account for the observed N atomic density in the film. Therefore, we expect that Si atoms are delivered to the surface via SiH_x radicals creating an amorphous silicon like film that is nitrided by N and NH_2 radicals.

ACKNOWLEDGMENTS

The authors thank M. J. F. van de Sande, J. F. C. Jansen, A. B. M. Hüsken, and H. M. M. de Jong for their skilful technical assistance. C. C. H. Lamers is gratefully acknowledged for her contribution to the measurements. This study has been supported by the Netherlands Foundation for Fundamental Research on Matter (FOM) and by the Netherlands Ministry of Economic Affairs, the Ministry of Education, Culture and Science and the Ministry of Public Housing, Physical Planning and Environment (E.E.T. project "HR-CEL"). The research of one of the authors (W. M. M. K.) has been made possible by a fellowship of the Royal Netherlands Academy of Arts and Sciences (KNAW).

[1] J. C. Barbour, H. J. Stein, O. A. Popov, M. Yoder, and C. A. Outten, J. Vac. Sci. Technol. A **9**, 480 (1991).
[2] S. Garcia, I. Martil, G. Gonzalez, E. Castan, S. Duenas, and M. Fernandez, J. Appl. Phys. **83**, 332 (1998).
[3] J. M. Jeon and J.-L. Lee, Appl. Phys. Lett. **86**, 172101 (2005).
[4] D. Stryahilev, A. Sazonov, and A. Nathan, J. Vac. Sci. Technol. A **20**, 1087 (2002).
[5] A. G. Aberle, Sol. Energy Mater. Sol. Cells **65**, 239 (2001).
[6] J. Hong, W. M. M. Kessels, W. J. Soppe, A. W. Weeber, W. M. Arnoldbik, and M. C. M. van de Sanden, J. Vac. Sci. Technol. B **21**, 2123 (2003).
[7] N. I. Fainer, Yu. M. Rumyantsev, M. L. Kosinova, G. S. Yurjef, E. S. Maximovskii, and F. A. Kuznetsov, Appl. Surf. Sci. **113/114**, 614 (1997).
[8] X.-J. Liu, Y.-F. Chen, H.-L. Li, X.-W. Sun, and L.-P. Huang, Thin Solid Films **479**, 137 (2005).
[9] R. Di Mundo, R. d'Agostino, F. Fracassi, and F. Palumbo, Plasma Processes Polym. **2**, 612 (2005).
[10] G. Lucovsky, P. D. Richard, D. V. Tsu, S. Y. Lin, and R. J. Markunas, J. Vac. Sci. Technol. A **4**, 681 (1986).
[11] D. L. Smith, A. S. Alimonda, C.-C. Chen, S. E. Ready, and B. Wacker, J. Electrochem. Soc. **137**, 614 (1990).
[12] S. Sitbon, M. C. Hugon, B. Agius, F. Abel, J. L. Courant, and M. Puech, J. Vac. Sci. Technol. A **13**, 2900 (1995).
[13] D. Landheer, N. G. Skinner, T. E. Jackmann, D. A. Thompson, J. G. Simmons, D. V. Stevanovic, and D. Khatamian, J. Vac. Sci. Technol. A **9**, 2594 (1991).
[14] D. L. Smith, A. S. Alimonda, and F. J. von Preissig, J. Vac. Sci. Technol. B **8**, 551 (1990).
[15] B. F. Hanyaloglu and E. S. Aydil, J. Vac. Sci. Technol. A **16**, 2794 (1998).
[16] W. M. M. Kessels, F. J. H. van Assche, J. Hong, D. C. Schram, and M. C. M. van de Sanden, J. Vac. Sci. Technol. A **22**, 96 (2004).
[17] W. M. M. Kessels, F. J. H. van Assche, P. J. van den Oever, and M. C. M. van de Sanden, J. Non-Cryst. Solids **338**, 37 (2004).
[18] D. L. Smith, J. Vac. Sci. Technol. A **11**, 1843 (1993).
[19] D. B. Beach and J. M. Jasinski, J. Phys. Chem. **94**, 3019 (1990).
[20] D. T. Murley, R. A. G. Gibson, B. Dunnett, A. Goodyear, and I. D. French, J. Non-Cryst. Solids **187**, 324 (1995).
[21] J. A. Theil, S. V. Hattangady, and G. Lucovsky, J. Vac. Sci. Technol. A **10**, 719 (1992).
[22] H. Umemoto, T. Morimoto, M. Yamawaki, Y. Masuda, A. Masuda, and H. Matsumura, Thin Solid Films **430**, 24 (2003).
[23] E. R. Fisher, P. Ho, W. G. Breiland, and R. J. Buss, J. Phys. Chem. **96**, 9855 (1992).
[24] P. R. McCurdy, C. I. Butoi, K. L. Williams, and E. R. Fisher, J. Phys. Chem. B **103**, 6919 (1999).
[25] M. L. Steen, K. R. Kull, and E. R. Fisher, J. Appl. Phys. **92**, 55 (2002).
[26] S. F. Adams and T. A. Miller, Plasma Sources Sci. Technol. **9**, 248 (2000).
[27] H. Singh, J. W. Coburn, and D. B. Graves, J. Appl. Phys. **88**, 3748 (2000).
[28] P. J. van den Oever, J. L. van Hemmen, J. H. van Helden, D. C. Schram, R. Engeln, M. C. M. van de Sanden, and W. M. M. Kessels, Plasma Sources Sci. Technol. **15**, 546 (2006).
[29] B. Hoex, A. J. M. van Erven, R. C. M. Bosch, W. T. M. Stals, M. D. Bijker, P. J. van den Oever, W. M. M. Kessels, and M. C. M. van de Sanden, Prog. Photovoltaics **13**, 705 (2005).
[30] M. Schaepkens, T. W. Kim, A. G. Erlat, M. Tan, K. W. Flanagan, C. M. Heller, and P. A. McConnelee, J. Vac. Sci. Technol. A **22**, 1716 (2004).
[31] W. M. M. Kessels, C. M. Leewis, M. C. M. van de Sanden, and D. C. Schram, J. Appl. Phys. **86**, 4029 (1999).
[32] M. C. M. van de Sanden, R. J. Severens, W. M. M. Kessels, R. F. G. Meulenbroeks, and D. C. Schram, J. Appl. Phys. **84**, 2426 (1998); **85**, 1243 (1999).
[33] P. J. van den Oever, J. H. van Helden, C. C. H. Lamers, R. Engeln, D. C. Schram, M. C. M. van de Sanden, and W. M. M. Kessels, J. Appl. Phys. **98**, 093301 (2005).
[34] J. P. M. Hoefnagels, Y. Barrell, W. M. M. Kessels, and M. C. M. van de Sanden, J. Appl. Phys. **96**, 4094 (2004).
[35] W. M. M. Kessels, A. Leroux, M. G. H. Boogaarts, J. P. M. Hoefnagels, M. C. M. van de Sanden, and D. C. Schram, J. Vac. Sci. Technol. A **19**, 467 (2001).
[36] S. Agarwal, G. W. W. Quax, M. C. M. van de Sanden, D. Maroudas, and E. S. Aydil, J. Vac. Sci. Technol. A **22**, 71 (2004).
[37] J. Benedikt, S. Agarwal, D. Eijkman, W. Vandamme, M. Creatore, and M. C. M. van de Sanden, J. Vac. Sci. Technol. A **23**, 1400 (2005).
[38] A. Goumri, W.-J. Yuan, L. Ding, Y. Shi, and P. Marshall, Chem. Phys. **177**, 233 (1993).
[39] L. G. Piper and G. E. Caledonia, J. Phys. Chem. **95**, 698 (1991).
[40] A. H. Mahan, A. C. Dillon, L. M. Gedvillas, D. L. Williamson, and J. D. Perkins, J. Appl. Phys. **94**, 2360 (2003).
[41] Q. Wang, S. Ward, L. Gedvilas, B. Keyes, E. Sanchez, and S. Wang, Appl. Phys. Lett. **84**, 338 (2004).
[42] S. G. Ansari, H. Umemoto, T. Morimoto, K. Yoneyama, A. Izumi, A. Masuda, and H. Matsumura, Thin Solid Films **501**, 31 (2006).
[43] A. I. Chowdhury, T. M. Klein, T. M. Anderson, and G. N. Parsons, J. Vac. Sci. Technol. A **16**, 1852 (1998).
[44] H. Motz and H. Wise, J. Chem. Phys. **32**, 1893 (1960).
[45] G. Ganguly and A. Matsuda, Phys. Rev. B **47**, 3661 (1993).
[46] Y.-K. Kim and J. P. Desclaux, Phys. Rev. A **66**, 012708 (2002).
[47] H. M. Rosenstock, K. Draxl, B. W. Steiner, and J. T. Herron, *Energetics of Gaseous Ions*, Journal of Physical and Chemical Reference Data, Vol. 6, Supplement No. 1 (American Institute of Physics, Melville, New York, 1977).

Downloaded 14 Sep 2007 to 131.155.108.71. Redistribution subject to AIP license or copyright, see http://jap.aip.org/jap/copyright.jsp